

Study on Thermal-Fluid-Solid Coupling Characteristics for Helicopter Intermediate Spiral Bevel Gear Reducer

Dongping Sheng*, Jie Yang, Chun Su

Master College of Mechanical Engineering, Changzhou Institute of Technology,
Changzhou, 213032, China

*Corresponding author: shengdp@czu.cn

Article history:

Received: 15 June 2024 / Received in revised form: 15 October 2024 / Accepted: 23 October 2024

Available online 28 October 2024

ABSTRACT

In the helicopter transmission system, the intermediate reducer is particularly special. It uses bevel gear pairs to change the transmission direction and to transfer the rotational speed effectively. Therefore, an in-depth study of the spiral gear pair is crucial to improve the overall performance of the helicopter rotor system. This study focuses on the study of the thermal-fluid-solid coupling characteristics and one-way steady-state thermal finite element analysis are conducted based on volume of fluid multiphase flow simulation theory to provide strong support for the design and optimization of the helicopter intermediate reducer. Several conclusions could be obtained. Firstly, it could be found that the negative pressure of the gear engagement occurs and the absolute value increases with the rotation speed of the gear moving wall in the flow field. Secondly, the effect force such as the gear decreases with the increase of the rotational speed of the gear moving wall in the flow field. Thirdly, the contact stress could be affected significantly at different working speed while considering the thermal-fluid influence; Finally, by reasonably controlling the speed of the gear, the stress level between the teeth can be reduced while ensuring the transmission efficiency, as well as improving the service life and reliability of the gear reducer.

Copyright © 2024. Journal of Mechanical Engineering Science and Technology.

Keywords: FEA, helicopter, one-way, spiral bevel gear, thermal-fluid-solid coupling

I. Introduction

The helicopter occupies a pivotal position in the modern aviation industry, its unique vertical take-off and landing and air hover ability, without relying on the airport runway, so that it has shown a high practical value in the military, civil and police fields. Especially in military applications, helicopters play an irreplaceable role. In the helicopter transmission system, the intermediate reducer is particularly special. It usually uses spiral bevel gears to change the direction of transmission and effectively transfer the speed. Therefore, the in-depth study of spiral bevel gear is very important to improve the overall performance of helicopter rotor system. By optimizing the design of spiral bevel gear, the transmission efficiency of helicopter can be further improved and the energy loss can be reduced, so as to enhance the overall performance of helicopter.

The earliest research about fundamental geometrical characteristics of bevel gears was discussed in 1984 [1]. In this study, the mathematical modeling of the tooth surface geometry of bevel gears can be developed based on the basic gearing kinematics and involute geometry along with the tangent plane geometry. Furthermore, the parametric representations of the spherical involute and the involute spirilloid is derived as well. In 1992, The best geometry of a gear set usually was found by varying the parameters of most



influence within reasonable bounds, and the parameters varied were the number of teeth of the pinion and of the gear, the spiral angle, sum of pressure angles, and others [2]. The influence of train speed on the equilibrium temperature of the practical spur gear was studied to suit for the development of high-speed train, and it is found the equilibrium temperature increases with the increase of train speed [3]. A novel modeling approach for studying the lateral lubricating gap between sliding lateral bushes and spur gears in external gear machines was presented, and it is found that pressure compensated lateral bushings were important design elements for efficient operation of an external gear pump or motor [4]. A fluid structure interaction model for the simulation of the flow in the lubricating gaps between gears and lateral bushes in external gear machines was presented, and the proposed model was capable of accounting for elasto-hydrodynamic effects in the lubricant film, and can predict the lubricant film thickness [5]. A computational fluid dynamics (CFD) model based on the finite volume method (FVM) was built to investigate the oil distribution and the churning losses inside a single-stage gearbox of the FZG back-to-back efficiency gear test rig. Thereby, a three-dimensional finite volume simulation model considering two-phase flow was applied [6]. A six-degree-of-freedom tribo-dynamics model for spur gear pair was proposed based on the load sharing theory and dynamics theory, Time-varying mesh stiffness and film stiffness, surface roughness as well as the friction torque were considered for establishing the model [7]. Three-dimensional analysis of unsteady state temperature field and temperature sensitivity analysis of gear transmission was investigated, for which frictional heat caused surface temperature rise which reduced their bearing capacity and scuffing resistance. Unsteady-state temperature field of gear surface was analyzed and results providing continuous temperature distribution of any meshing moment and at any position on gear surface [8]. To determine the temperature rise of the tooth surface as a result of the friction heat in mixed elastohydrodynamic lubrication (EHL), a coupled thermo-elasto-hydrodynamic analysis was carried out in consideration of the load shearing, mixed lubrication characteristics, heat generation in the contact region [9]. A finite volume CFD model of a dip-lubricated planetary test gearbox was developed which includes the modelling of all gear meshes and bearings and has a very high level of detail. The element number was reduced as far as reasonable possible, resulting in little computing time with regard to the modeling depth [10]. The lubricating oil distribution and the internal pressure variation during gear engagement in the high-speed train unit gearbox were analyzed, and the volume of fluid (VOF) two-phase flow model based on fluid-structure interaction theory was established by using Reynolds-averaged Navier-Stokes (RNG) turbulence model and moving mesh model. The flow field was simulated and the pressure of key positions was monitored [11]. To improve the simulation and calculation accuracy of high-speed train driving gearbox temperature field and provide the support for the improving effect evaluation of lubricating oil flow channel structure, structural characteristics and lubrication method of high-speed train driving gearbox, the heat sources and heat dissipation route were analyzed [12]. To study the internal flow field and temperature field of the oil-immersion lubrication gearbox, RNG model. VOF model and dynamic mesh model were used to simulate the internal flow field of the gearbox. The steady-state temperature field of gearbox was simulated by using moving reference frame (MRF) model [13]. A computational fluid dynamics method to study the lubrication and temperature characteristics of an intermediate gearbox with splash lubrication was proposed, and a volume of fluid multi-phase model was used to track the interface between oil and air. A multiple reference frame model was adopted to accurately simulate the movement characteristics of the gears, bearings, and the surrounding flow field [14]. A complete three-dimensional CFD with conjugate heat transfer (CHT) model of an Electric Motor, including all the important parts like the windings, rotor

and stator laminate, end rings etc. Was created. The multi-phase volume of fluid approach was used to model the oil flow inside this motor [15]. A shroud was introduced to enclose the high-speed unmeshed spiral bevel gear. By leveraging the CFD software and selecting multi reference frame, the windage behavior of our proposed model was evaluated and compared with that without a shroud, and the influence of rotational speed of the bevel gear on windage power loss was also analyzed [16]. A numerical approach based on CFD for the prediction of lubricant fluxes and power losses of gearboxes was presented, and the presented methodology utilized a meshing strategy that reduces the computational effort of the simulations and enables parametrical studies [17]. To reduce the power losses, a computational fluid dynamics simulation technique that analyzes oil churning and windage losses was developed and improvements were made to the shrouds of bevel gears, which have large losses in the gearbox [18]. A computational fluid dynamics simulation technique that analyzes oil churning and windage losses was developed and improvements were made to the shrouds of bevel gears, which have large losses in the gearbox [19]. A numerical simulation model of the flow field in a gearbox with an oil volume adjusting device was established for the first time to study its influence on the lubrication characteristics of a high-speed electric multiple unit [20]. A CFD model based on the Finite Volume Method was built to investigate the oil distribution and the churning losses inside a single-stage gearbox [21]. The stiffness load ratio of the cracked tooth and the surrounding tooth was derived to study the temperature field of the gear transmission system with cracks [22]. A coupled thermo-elastic 3D finite element model has been developed to analyze the frictional heat generation and transient thermal behavior of spiral bevel gears [23]. A numerical method, which integrated the mixed elasto-hydro-dynamic lubrication model with a finite element method, was proposed based on thermal analysis [24]. Besides, the linear and nonlinear analysis based on finite element method (FEM) should be set correctly. The strain comparison of a pressure vessel made of HSLA 15CDV6 in a cylindrical shell membrane region in a pressure test was discussed [25]. Mechanics of pouch cell due to internal pressure was performed by elasto-plastic finite element structural analysis [26]. To prevent this gas entry, a spiral wound gasket was worked out to prevent the gas entry, and its design, thermo-structural analysis and effect on the system were presented [27].

Although a large number of research has been done about CFD of gear transmission, but there is no available literature about spiral bevel gear's thermal-fluid-solid coupling characteristics. In this paper, a parametric model of circular spiral bevel gear of helicopter intermediate reducer is established, and based on this model, the influence of lubricating oil and wall speed of spiral bevel gear on the medium effect force of spiral bevel gear structure field is analyzed under the condition of constant oil temperature.

II. Material and Methods

Physical Model

It is necessary to know that two types of spiral bevel gear system including Orlikon and Gleason while discussing the design and analysis of gear transmission system. For the traditional Gleason spiral bevel gear modeling method, it relies on the known gear parameters and meshing principle to construct the tooth surface equation. When the spiral bevel gear model is constructed, the tooth surface equation is used to generate the tooth surface data points, and the tooth surface meshing is realized through these data points. But this approach requires both deep expertise and heavy data processing, making it difficult to

popularize in practical applications. Therefore, it is of practical significance to develop a simple and efficient method for modeling and performance analysis of spiral bevel gear.

The parameters of spiral bevel gear are obtained based on a kind of helicopter intermediate reducer. The transmission ratio is 1.31 and the gear tooth number of drive gear is 29. Additionally, the shaft angle is set to be 126 degrees, and the Gleason kind of spiral bevel gear is adopted. Based on the setting above, the parametric model of spiral bevel gear of a kind of helicopter intermediate reducer is established and 3D model is built, as shown in Figure 1.

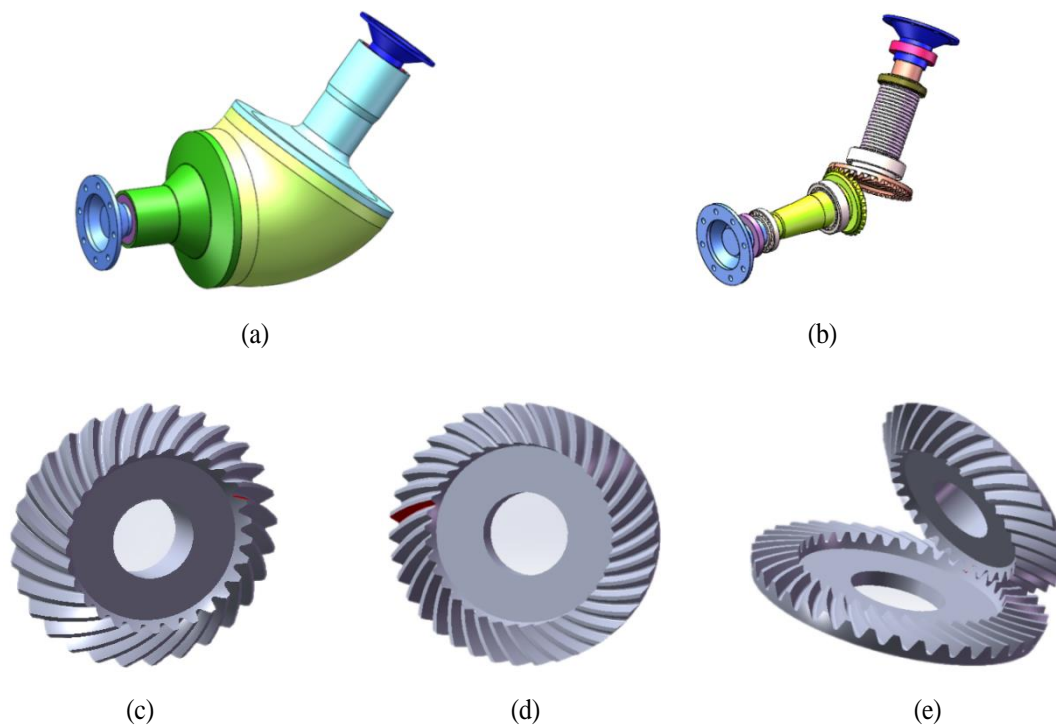


Fig.1. Spiral bevel gear model of helicopter intermediate reducer: (a) Overview of gear reducer; (b) Internal view of gear reducer; (c) Drive gear; (d) Passive gear; (e) Gear meshing pair

Thermal-fluid-solid Analysis Procedure

Figure 2 shows the thermal-fluid-solid optimization analysis flow chart and algorithm for helicopter intermediate spiral bevel gear reducer. As can be seen from Figure 2, the design parameters of the spiral bevel gear reducer need to be extracted and set as the variables to conduct the optimization analysis. Besides, the boundary conditions for each analysis should be inputted correctly based on ANSYS Software.

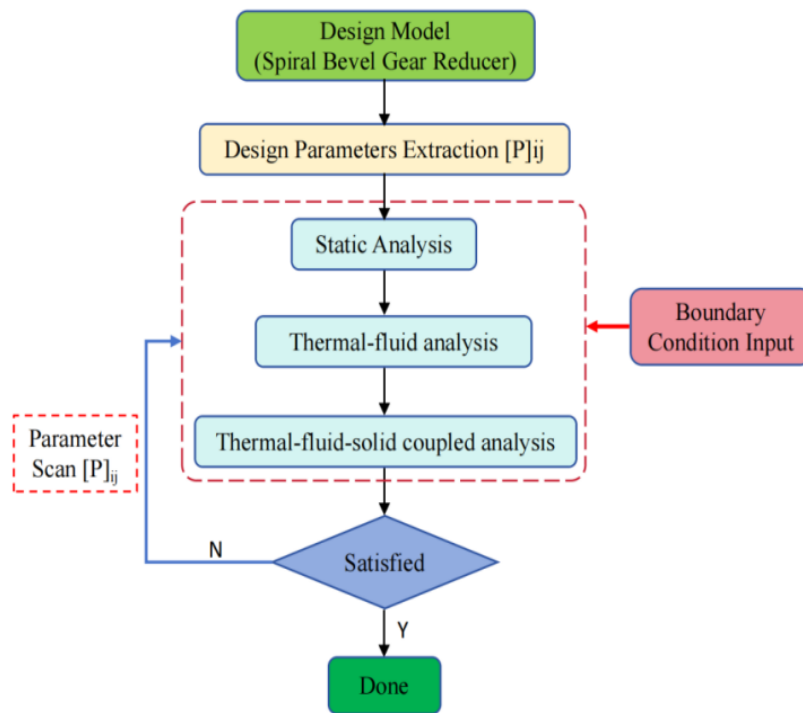


Fig. 2. Thermal-fluid-solid analysis flow chart for helicopter intermediate spiral bevel gear reducer

III. Results and Discussions

Thermal-Fluid-Solid Coupling Analysis

A. Static analysis

Static analysis is the basis of the thermal-fluid-solid coupling research, and the characteristics of the spiral bevel gear system under the specified torque is obtained. The gear's material is set to be 40Cr and the related mechanical data is set in system as well as the stress-strain curve. On the other hand, related boundary condition is set based on the local cylindrical coordinates and the nodes located on the inner hole of the both spiral gears have five degrees except freedom of radial displacement, as shown in Figure 3. The meshed model, frictional contact pairs, torque load condition and so on could be seen in Figure 3. At the same time, to make sure the stress result is accurate, the nonlinear contact analysis is conducted although this nonlinear analysis could lead to long iterative calculations, and section B and C have the same setting as well.

Besides, it should be noted that, as the complex structure shape, the tetrahedron element is adopted. At the same time, based on the consideration of time cost and result accuracy, several rough calculations under the different element size are conducted, and 2mm element dimension is chosen finally for this model, which could lead to a converged result and no better result could be obtained when smaller element is set. The models in section B and C are meshed with the same size.

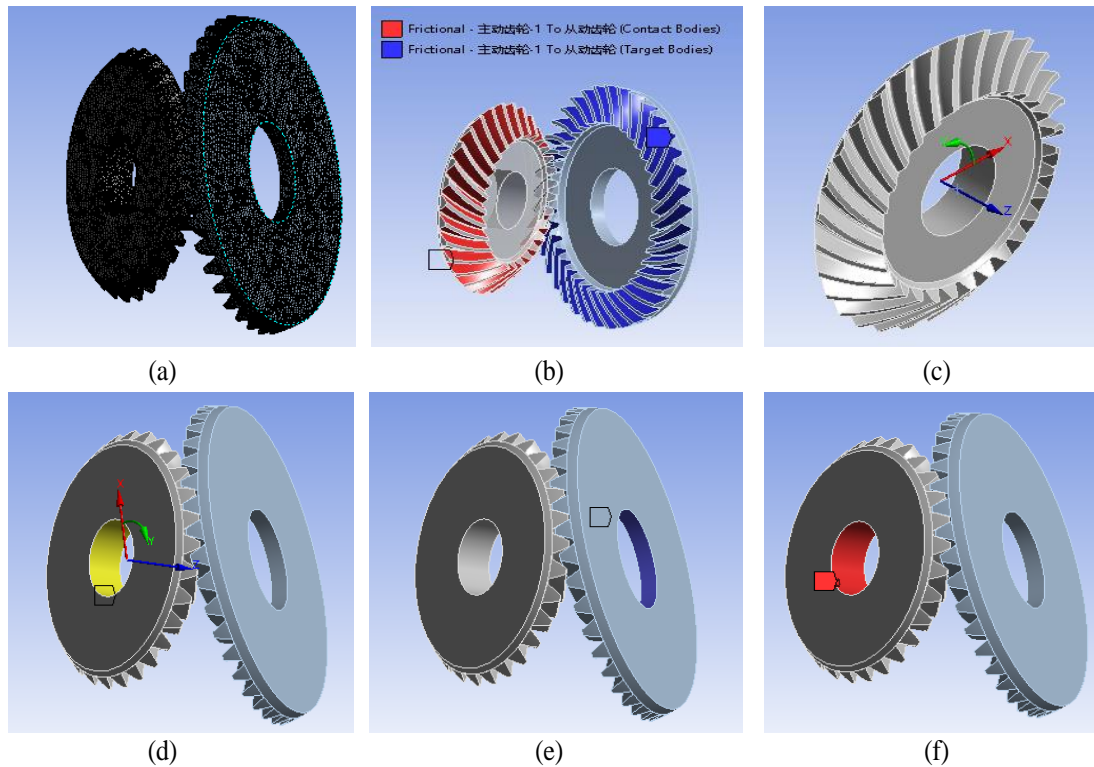


Fig.3. Boundary condition: (a) Meshing model; (b) Contact setting; (c) Coordinate setting; (d) Drive gear's boundary condition; (e) Passive gear's boundary condition; (f) Load setting

Figure 3. Boundary condition: (a) Meshing model; (b) Contact setting; (c) Coordinate setting; (d) Drive gear's boundary condition; (e) Passive gear's boundary condition; (f) Load setting.

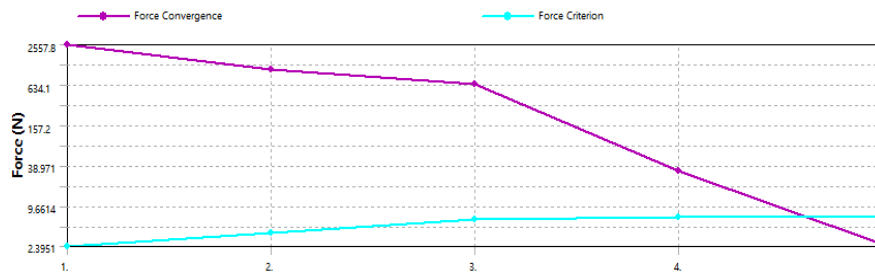


Fig.4. Convergence curve

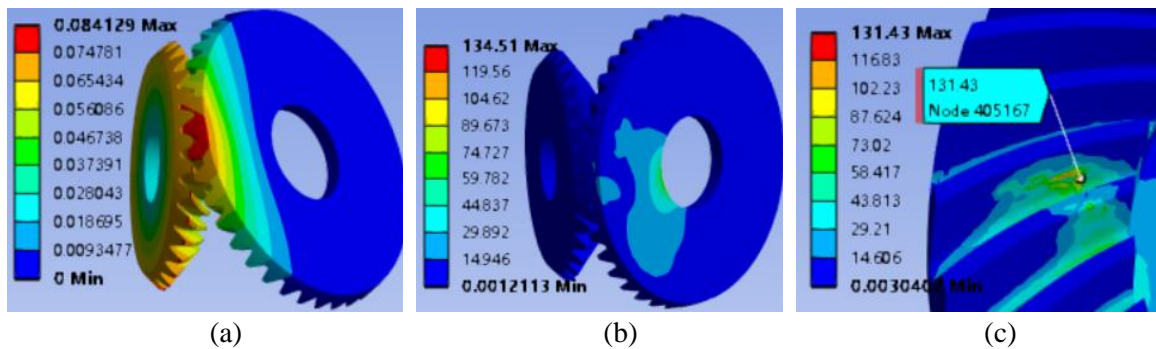


Fig.5. Static result: (a) Deformation distribution (mm); (b) Stress distribution (MPa); (c) Local contact stress (MPa)

B. Thermal-fluid Analysis

The gear box model is simplified, the fluid domain around the gear is created, and the steady-state fluid flow is analyzed by VOF multiphase flow simulation tool. The VOF model is a numerical method used to simulate the interfacial flow of a variety of immiscible fluids. The core idea of this model is to take the Volume Fraction of the fluid in the computational domain as the main parameter for tracing the fluid interface. Through this integral number segment, different fluids can be represented and distinguished in a numerical computation grid.

The VOF model is widely used in the calculation of multiphase flow, such as gas-liquid two-phase flow, oil-water mixed flow and so on. Its general applications include slosh, the flow of large bubbles in liquids, and the determination of the steady or instantaneous interface of any liquid-gas interface. In addition, the VOF model also needs to consider the conservation of mass and momentum of the fluid to ensure the accuracy of the simulation. In the VOF model, the physical quantity on the interface is not solved directly, but the whole fluid conservation equation is solved, and the interface position is identified by the specific interface reconstruction technology. It is worth noting that the VOF model mainly focuses on the multiphase flow problem under unstable conditions. Although it is used to describe dynamic changes in flow in most cases, it can also meet the steady-state requirements of some multiphase flow models in specific application scenarios. Steady-state VOF calculation is meaningful only when the solution is not affected by the initial conditions and each phase has an obvious inflow boundary.

For the analysis in this paper, the oil inlet is created above the engagement of the bevel gear, and the oil outlet is created below. The Boolean subtraction operation is first performed to subtract the solid domain (bevel gear pair) from the fluid domain, and the subtracted model is retained. Note that if the bevel gear pair interferes seriously, it will cause the Boolean operation to fail, and even if the Boolean operation can be performed, it will report an error when dividing the grid. Then, the fluid domain and the solid domain are conodal coupled to prepare for the temperature and pressure load to be inserted later, and the inlet, outlet and wall surface are named. Only the wall surface of the gear in the fluid domain can be named, and the driving gear is first hidden in the naming, and the driven gear surface is selected for naming. After that, tetrahedral mesh is used, as shown in Figure 6 and Figure 7.

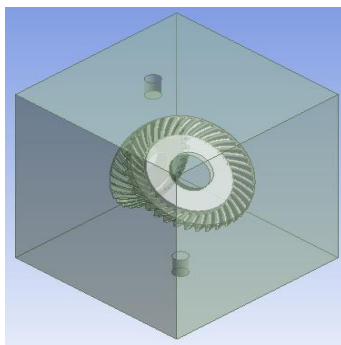


Fig.6. 3D model with fluid

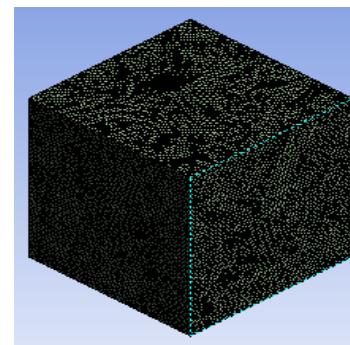
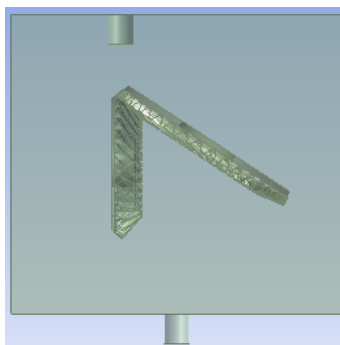


Fig.7. Meshed 3D model with fluid

Additionally, the unites need to be changed in to millimeters, and the meshing need to be checked to make sure that no negative volume of the grid appears, set the gravity to 9.81m/s^2 in the negative Y-axis direction, open the energy equation, and use the standard k-epsilon turbulence model and the standard wall function. Set the material. The lubricating oil material is shown in Table 1.

Table 1. Lubricating oil parameters

| Parameter | Value |
|--|--------|
| Density ($\text{kg}\cdot\text{m}^{-3}$) | 870 |
| Specific heat ($\text{J}\cdot(\text{kg}\cdot\text{K})^{-1}$) | 2077 |
| Thermal conductivity ($\text{W}\cdot(\text{m}\cdot\text{K})^{-1}$) | 0.1454 |
| Dynamic viscosity ($\text{kg}\cdot(\text{m}\cdot\text{s})^{-1}$) | 0.087 |

Setting the air as the first phase, the lubricating oil as the second phase, and the lubricating oil temperature equals 340K. In general, the working temperature of gear oil should be controlled in the range of 60 to 90 centigrade. In this temperature range, the gear oil can not only ensure the lubrication performance but also ensure the normal operation of the gear transmission, so as to achieve long-term stable operation. Checking the surface tension model and wall adhesion, and the surface tension coefficient between lubricating oil and air is 0.04. Besides, a local coordinate system needs to be created based on the center of gravity coordinates of the passive wheel, which is equivalent to the X axis by 54° counterclockwise about the Z axis. Inlet speed is set to be 3m/s and the oil volume fraction to 1. The driving wheel wall in the fluid domain is set as a moving wall, rotated relative to the absolute coordinate system. Additionally, the rotation center is the center of gravity of the driving wheel, the rotation axis is expressed based on the X-axis unit vector (1,0,0), and the speed is set to be 50 rad/s.

The pressure-velocity coupling method was used, the Least squares cell based discrete gradient suitable for turbulence was adopted, the pressure interpolation method was PRESTO, the momentum dispersion was selected as the second-order upwind scheme, the standard initialization was selected. The initial temperature was changed to 298.15K, and the initial volume fraction of lubricating oil was 0. By the same way, the results of other four sets of driving wheel speed including 100 rad/s, 150 rad/s, 200 rad/s, and 250 rad/s are obtained, and the results are shown in Figure 8.

Based on Figure 8, it could be found that the larger the speed, the smaller the coverage area of the lubricating oil, and the smaller the corresponding temperature range. This phenomenon is generated mainly by the reason that the higher speed could throw out more lubricating oil in the same time, and the area covered by the lubricating oil of gear is reduced correspondingly. However, it could be observed that no matter how much changes of the speed, the lubricating oil will cover the gear meshing area all the time, and the temperature caused by the lubricating oil has little effect on the stress at the meshing area under different speeds, which could be concluded that so the key factor of causing the stress change at the gear meshing area is the change of the pressure.

The velocity cloud image at different velocity and the velocity vector of the driving gear are obtained and shown in Figure 9. The speed of the two gears increases gradually from the inner ring to the outside and is distributed in a gradient, and the speed at the top of the outer tooth is the largest. From the speed vector diagram of different angular speeds, it can be seen that the color changes from mostly blue to mostly yellow, and the speed is gradually increasing. It can be seen from the static analysis that the gear meshing is not at the maximum speed. More importantly, considering the speed is distributed in gradient, the maximum speed can be used to represent the speed change trend at the gear meshing under different speeds. The above findings could be verified quantitatively and have the similar trend with the available study [23].

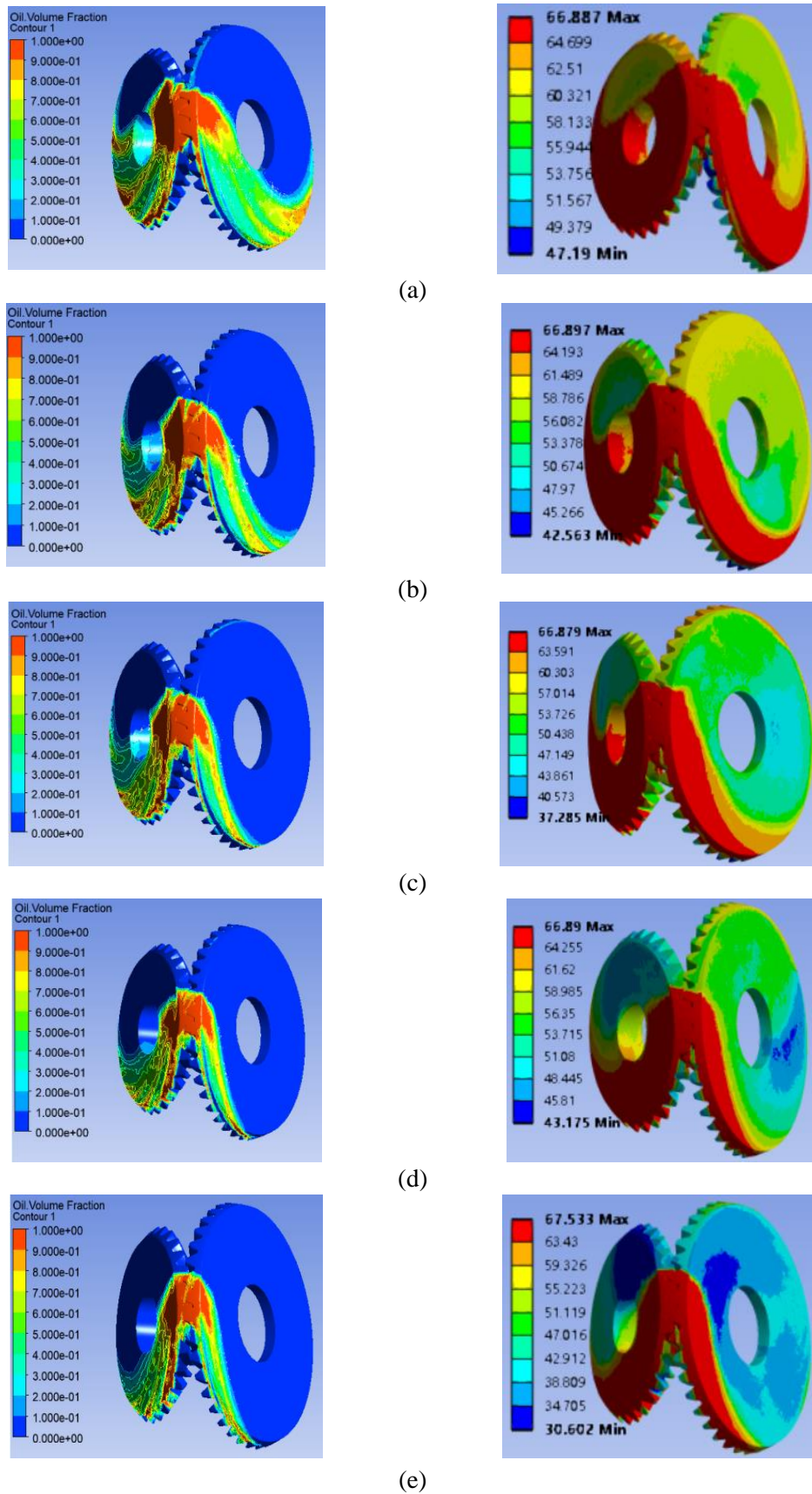


Fig. 8. Oil volume fraction and temperature cloud image at different rotational speeds: (a) 50 rad/s; (b) 100 rad/s; (c) 150 rad/s; (d) 200 rad/s; (e) 250 rad/s

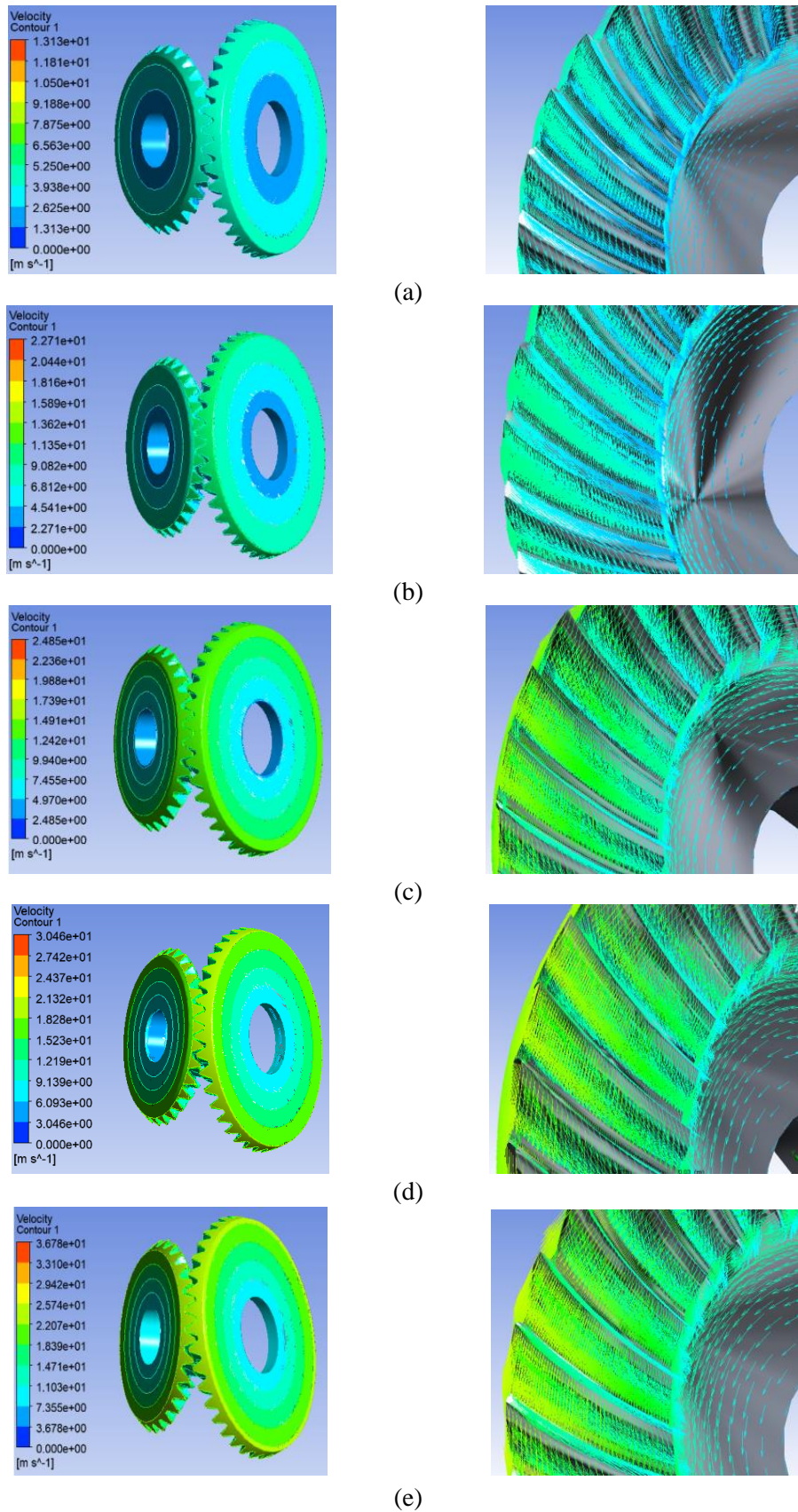


Fig. 9. The velocity cloud image at different velocity and the velocity vector of the driving gear: (a) 50 rad/s; (b) 100 rad/s; (c) 150 rad/s; (d) 200 rad/s; (e) 250 rad/s

Figure 10 shows the pressure cloud map at the engaging point of the driving wheel, and it could be clearly observed that negative pressure has occurred in some areas.

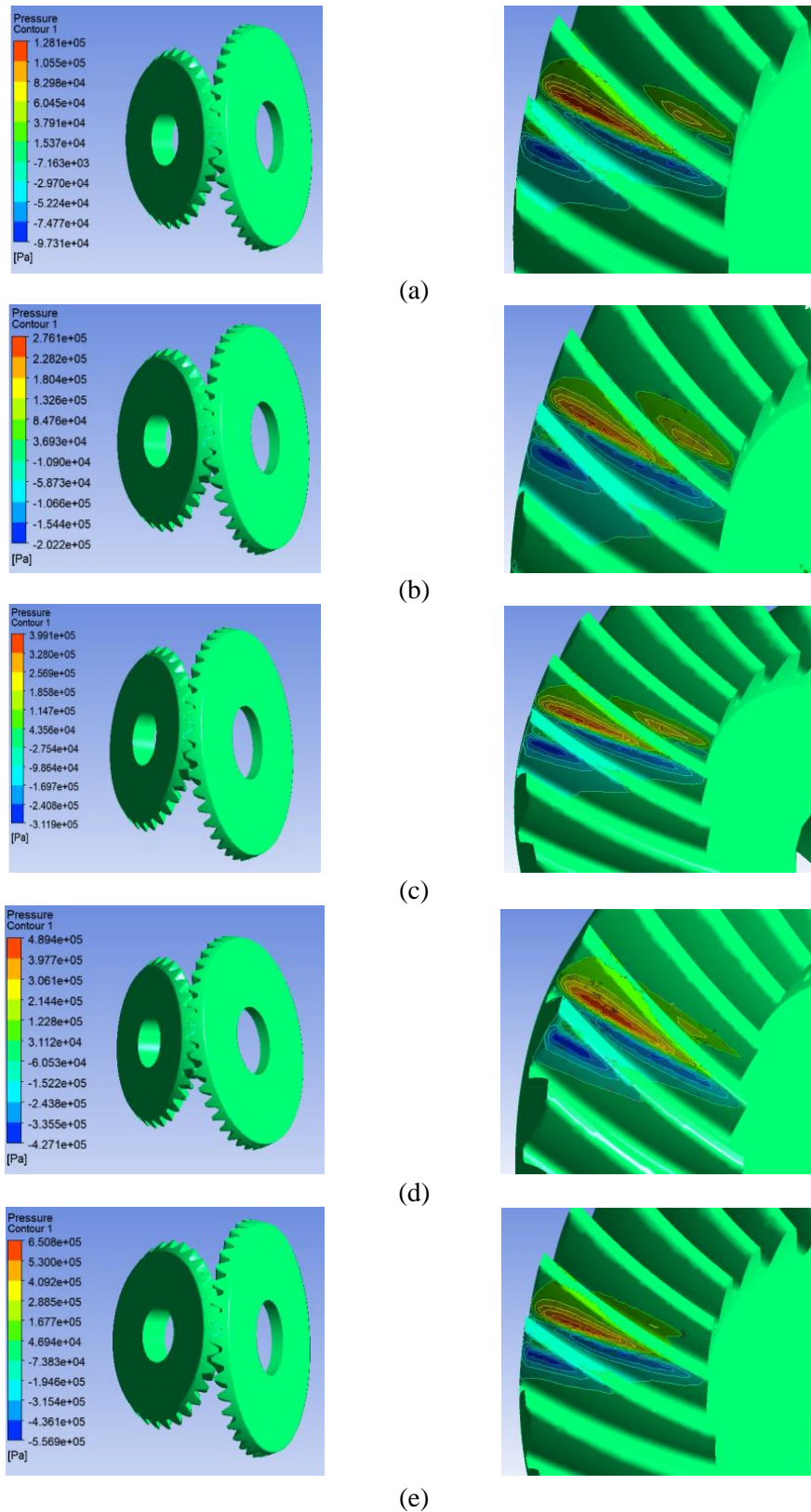


Fig.10. Pressure cloud under angular velocity and pressure cloud at the engagement of the driving wheel: (a) 50 rad/s; (b) 100 rad/s; (c) 150 rad/s; (d) 200 rad/s; (e) 250 rad/s

The formation of this negative pressure is somewhat similar to the working principle of gear pumps. In the process of gear transmission, when two adjacent teeth gradually separate from the meshing state, that is, the moment the gear meshes out, the space originally occupied by the teeth begins to gradually increase. Due to the inability of gas or lubricating oil in this space to quickly fill the increased volume, a local vacuum area is formed, resulting in the generation of negative pressure.

Some phenomena could be observed based on Figure 11 and Figure 12. When the outer teeth start to disengage (i.e. the gap between two adjacent teeth begins to increase), the inner teeth have completely engaged, and the outer teeth form a larger space, which is the direct cause of negative pressure generation. Meanwhile, the teeth inside the red circle represent the next tooth within the white circle that is ready to disengage. From the figure, it could be observed that when the outer end of the teeth inside the white circle begins to disengage, the teeth inside the red circle are also about to begin the disengagement process, forming a larger spatial volume and generating negative pressure. This continuous meshing and meshing process causes the volume of space between gears to constantly change, thus forming a negative pressure area. The formation of these negative pressure areas has a significant impact on the performance of gear transmission. They not only alter the stress distribution at the gear mesh, but may also affect the flow and lubrication effect of lubricating oil. Therefore, understanding and controlling the formation of these negative pressure areas is crucial for designing and optimizing gear transmission systems.

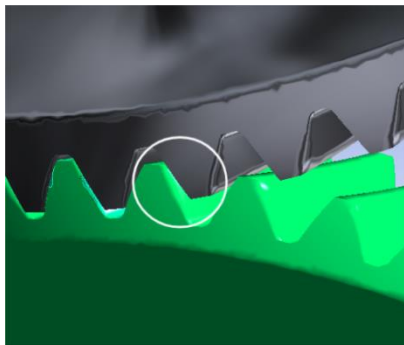


Fig.11. Local magnified view from outside end of the meshing out position

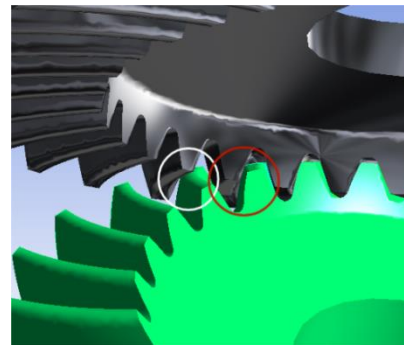


Fig.12. Local magnified view from inside end of the meshing out position

As the speed increases, as shown in Figure 13, the absolute value of negative pressure also gradually increases as well. By systematical analysis, with the increase of the speed, the frequency of gear meshing and meshing increases, which could result in an accelerated rate of change in the volume of space between gears. This rapid change makes it easier for local vacuum areas to form, and the absolute value of negative pressure also increases accordingly. This change not only increases the complexity of gear transmission, but may also have adverse effects on the stability and reliability of the system. Therefore, when designing and optimizing gear transmission systems, it is necessary to fully consider the impact of rotational speed on the negative pressure area and take corresponding measures to reduce its negative impact, which has the similar trend with the available research [24].

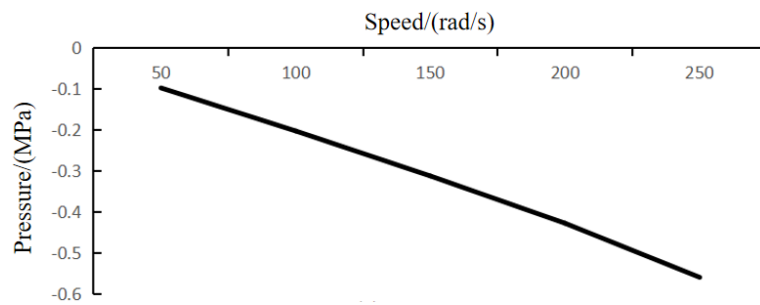


Fig. 13. Pressure line chart of speed vs. pressure

C. Thermal-fluid-solid Coupled Analysis

Base on the analysis caused by effect of thermal-fluid, the structure deformation and stress are conducted. Figure 14 shows the deformation cloud map at a certain torque and different speeds, and it could be found that there is not much difference in deformation at different speeds. The deformation is distributed in a gradient along the radial direction of the gear, with the maximum deformation at the gear meshing point and the minimum deformation at the inner ring of the gear.

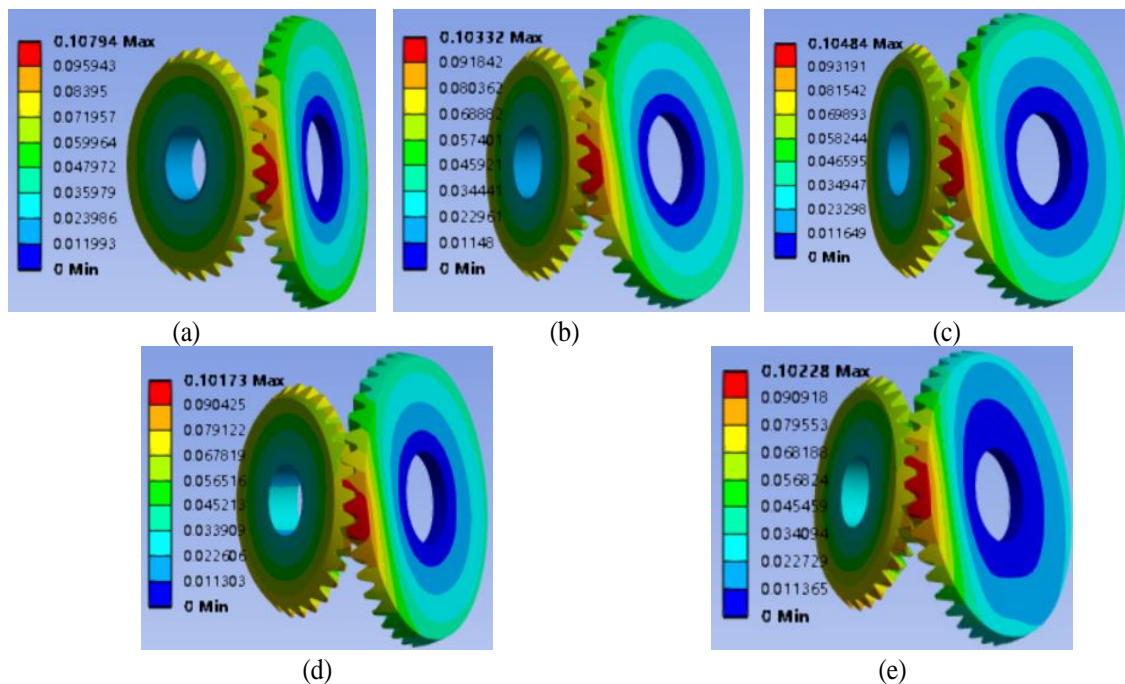


Fig. 14. Deformation under different rotating speed (mm): (a) 50 rad/s; (b) 100 rad/s; (c) 150 rad/s; (d) 200 rad/s; (e) 250 rad/s

Figure 15 shows the stress cloud map of the spiral bevel gear. As shown in the figure, the inner ring of the two gears experiences the highest stress, which is significantly different from the static analysis. The pressure on the inner ring of the gear is the same as that on the two end surfaces, so it must be caused by the influence of lubricating oil temperature. It should be due to stress concentration at the boundary of the inner ring, which is then transmitted to the entire surface of the inner ring.

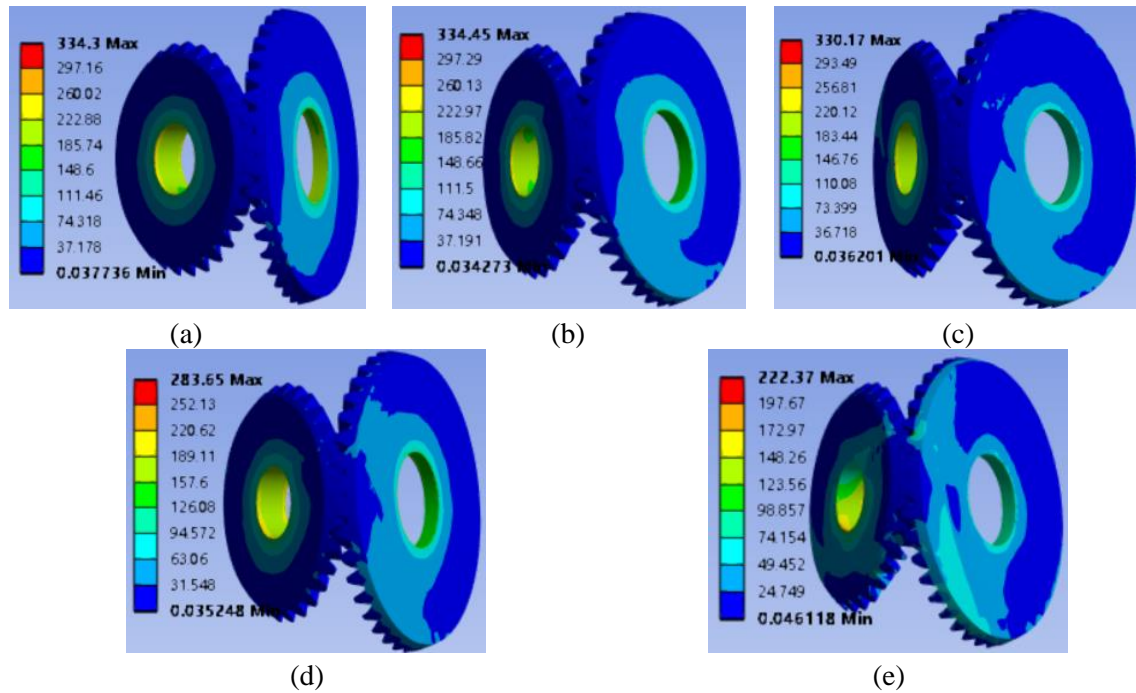


Fig.15. Equivalent stress distribution at different rotating speed (MPa): (a) 50 rad/s; (b) 100 rad/s; (c) 150 rad/s; (d) 200 rad/s; (e) 250 rad/s

Figure16 depicts the equivalent stress distribution at the meshing point of the driving wheel under different rotational speed conditions.

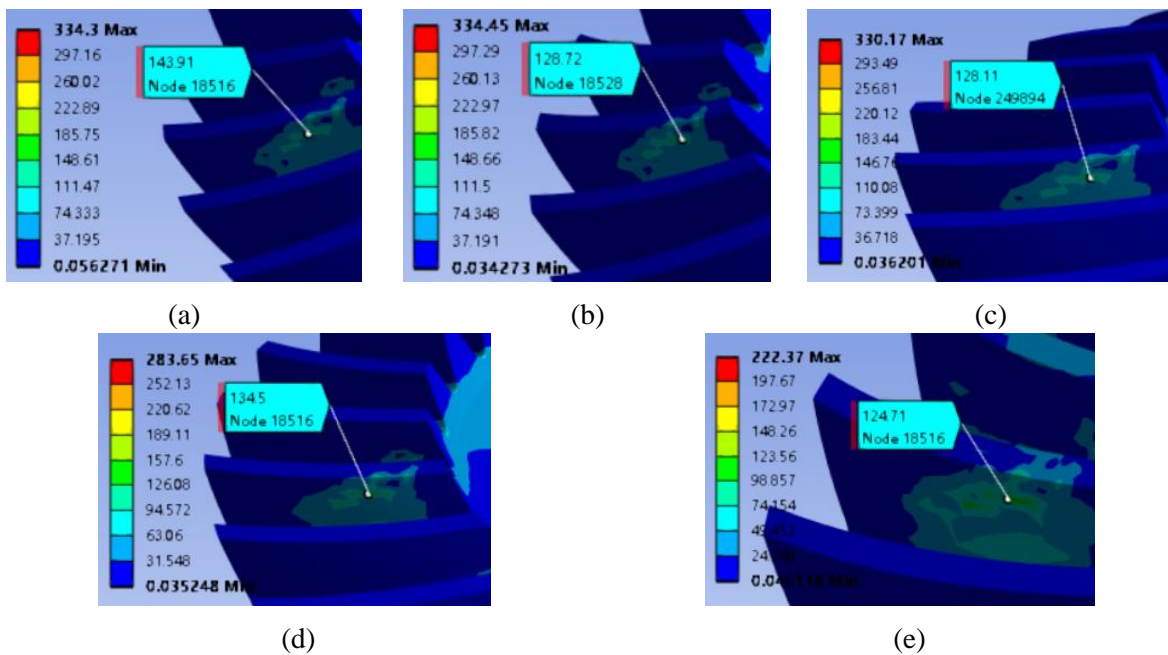


Fig.16. Equivalent stress distribution of driving gear at different rotating speed (MPa): (a) 50 rad/s; (b) 100 rad/s; (c) 150 rad/s; (d) 200 rad/s; (e) 250 rad/s

Stress distribution maps (Figure 16) show the stress concentration areas, stress distribution patterns, and stress levels of gears at specific speeds. This method can quickly identify which areas may face higher stress challenges during gear operation, guiding us to carry out targeted optimization and design. Additionally, by comparing the contact stress

under the condition of pure static and thermal-fluid affected analysis, as shown in Figure 5 and Figure 16 respectively, it could be found that, when system is under low-speed operation, the thermal-fluid could affect the contact stress significantly and increased about 6.7%. However, the change of contact stress is lowered when system runs at high-speed condition.

Furthermore, Figure 17 quantifies the relationship between the equivalent stress at the meshing point of the driving wheel and the rotational speed. It can be clearly seen from the graph that as the rotational speed increases, the equivalent stress at the meshing point of the driving wheel shows a decreasing trend. On the one hand, as the speed increases, the absolute negative pressure generated at the gear meshing gradually increases. In gear transmission systems, the formation of negative pressure is caused by the relative motion between tooth surfaces during gear meshing, resulting in changes in air pressure. The generation of this negative pressure has a certain lubrication and cooling effect on the gear meshing process, but it also affects the stress distribution between the tooth surfaces. Due to the increase in the absolute value of negative pressure, it will have a certain counteracting effect on the stress between the tooth surfaces, thereby reducing the equivalent stress at the meshing point of the driving wheel. On the other hand, as the rotational speed increases, the gear meshing frequency also increases. This means that the contact and separation process between tooth surfaces is more frequent, and the stress pulses generated by each contact and separation are also shorter. Although this high-frequency stress pulse can generate high stress peaks in a short period of time, due to its short duration, the cumulative damage to the material is relatively small. Therefore, overall, as the rotational speed increases, the equivalent stress at the meshing point of the driving wheel shows a decreasing trend.

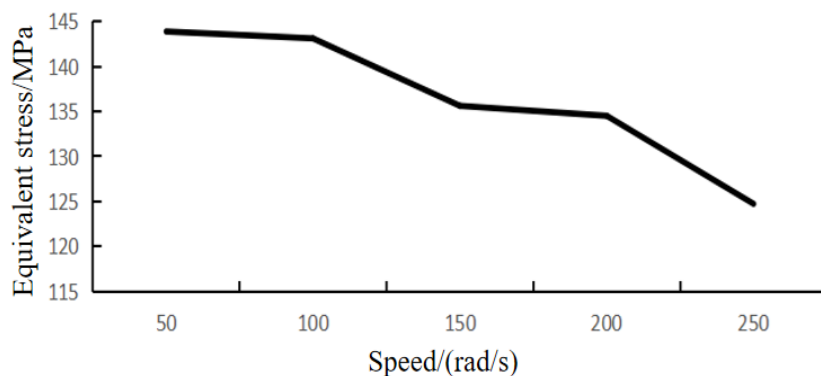


Fig.17. Equivalent stress curve under different rotating speed

IV. Conclusions

This paper focuses on the study of the thermal-fluid-solid coupling characteristics and one-way steady-state thermal finite element analysis are conducted based on VOF multiphase flow simulation theory to provide strong support for the design and optimization of the helicopter intermediate reducer. The following conclusions can be drawn from the analysis: (1) One-way steady-state heat-fluid-structure coupling finite element analysis of spiral bevel gear is carried out. It is found that with the increase of gear moving wall speed, negative pressure is generated in some areas at the engagement of the driving wheel, and the absolute value of negative pressure is increasing, and the equivalent stress at the engagement of the driving wheel is also decreasing; (2) With the increase of speed, the absolute value of negative pressure generated at the gear mesh gradually increases. In the gear transmission system, the formation of negative pressure is due to the relative motion between the tooth

surfaces during the gear meshing process, resulting in the change of air pressure. This negative pressure has a certain lubrication and cooling effect on the meshing process of the gear, but it also affects the stress distribution between the tooth surfaces. As the absolute value of negative pressure increases, it will have a certain counteracting effect on the stress between the tooth surfaces, thus reducing the equivalent stress at the engagement of the driving wheel; (3) The increase of speed means meshing frequency is increased as well as the contact and separation process between the tooth surfaces, and the stress pulse generated by each contact and separation is shorter. Although this high-frequency stress pulse will produce a high stress peak in a short time, due to its short duration, the cumulative damage to the material is relatively small. Therefore, on the whole, with the increase of speed, the equivalent stress at the engagement of the driving wheel shows a decreasing trend; (4) The contact stress under the condition of pure static and thermal-fluid affected analysis, it could be found that, when system is under low-speed operation, the thermal-fluid could affect the contact stress significantly and increased about 6.7%. However, the change of contact stress is lowered when system runs at high-speed condition; (5) By reasonably controlling the speed of the gear, the stress level between the tooth surfaces can be reduced while ensuring the transmission efficiency, thus improving the service life and reliability of the gear. In addition, for the gear drive system under specific working conditions, the speed can be adjusted according to actual needs to optimize the stress distribution and reduce the stress level; (6) Although the work done in this paper, the influences caused by several parameters including dynamic heat generation, sliding velocity and friction loss are not considered in this paper, which will be studied further in future works as well as the experimental research.

Acknowledgement

This work is Supported by National Key Laboratory of Science and Technology on Helicopter Transmission (Nanjing University of Aeronautics and Astronautics) (Grant No. HTL-O-20K01) and Changzhou Sci & Tech Program) (Grant No. CJ20240065).

References

- [1] Y. Tsai, and P. Chin, "Surface geometry of straight and spiral bevel gears," *ASME Journal of Mechanisms Transmissions and Automation in Design*, vol. 10, no. 12, pp. 133-134, 1984, doi: 10.1115/1.3258815.
- [2] L. Kohaupt, "Application of mathematical optimization in designing spiral bevel and hypoid gear blanks." *ZOR-Methods and Models of Operations Research*, vol. 10, no. 3, pp. 150-153, 1992, doi: 10.1007/BF01416247.
- [3] X.L. Chen, W.G. Zhang and Z.Y. Huang, "Influence of high-speed train running speed on transmission gear box equilibrium temperature," *Journal of Shanghai Jiao Tong University*, vol. 259, no. 9, pp. 1510-1513, 2007, doi: 10.3321/j.issn: 1006-2467. 2007.09.026.
- [4] S. Dhar, and A. Vacca, "A novel CFD-Axial motion coupled model for the axial balance of lateral bushings in external gear machines," *Simulation Modelling Practice and Theory*, vol. 26, pp. 60-76, 2012, doi: 10.1016/j.simpat.2012.03.008.
- [5] S. Dhar, and A. Vacca, "A fluid structure interaction-EHD model of the lubricating gaps in external gear machines: Formulation and validation," *Tribology International*, vol. 62, pp. 78-90, 2013, doi: 10.1016/j.triboint.2013.02.008.

- [6] H. Liu, T. Jurkschat and T. Lohner, "Determination of oil distribution and churning power loss of gearboxes by finite volume CFD method," *Tribology International*, vol. 109, pp. 346-354, 2016, doi: 10.1016/j.triboint.2016.12.042.
- [7] Y.J. Zhou, and D.G. Chang, "Coupling of dynamics and elasto-hydrodynamic lubrication for spur gear," *Journal of Aerospace Power*, vol. 31, no. 8, pp. 2010-2020, 2016, doi: 10.13224/j.cnki.jasp.2016.08.028.
- [8] L. Wei, and J. Tian, "Unsteady-state temperature field and sensitivity analysis of gear transmission," *Tribology International*, vol. 116, pp. 229-243, 2017, doi: 10.1016/j.triboint.2017.07.019.
- [9] J. Zhang, S. Liu and T. Fang, "Determination of surface temperature rise with the coupled thermo-elasto-hydrodynamic analysis of spiral bevel gears," *Applied Thermal Engineering*, vol. 124, pp. 494-503, 2017, doi: 10.1016/j.applthermaleng.2017.06.015.
- [10] H. Liu, P. Standl and M. Sedlmair, "Efficient CFD simulation model for a planetary gearbox," *Forsch Ingenieurwes*, vol. 82, no. 4, pp. 319-330, 2018, doi: 10.1007/s10010-018-0280-2.
- [11] C. Gao, K.L. Zhang and Y. Zhang, "Numerical study of the flow field of high-speed gearbox based on fluid-structure interaction theory," *Lubrication Engineering*, vol. 43, no. 8, pp. 69-75, 2018, doi: 10.3969/j.issn.0254-0150.2018.08.011.
- [12] H.H. Xu, J.L. Jiang and Y. Hu, "Modeling and simulation of steady-state temperature field of high-speed rail drive gear box," *Lubrication Engineering*, vol. 44, no. 9, pp. 44-49, 2019, doi: 10.3969/j.issn.0254-0150.2019.09.008.
- [13] H. Y. Bao, Y. Fan and R. P. Zhu, "Simulation analysis of flow field and temperature field of oil-immersion lubrication gearbox," *Journal of Central South University (Science and Technology)*, vol. 50, no. 08, pp. 1840-1847, 2019, doi: 10.11817/j.issn.1672-7207.2019.08.011.
- [14] F.X. Lu, M. Wang and W.B. Pan, "CFD-based investigation of lubrication and temperature characteristics of an intermediate gearbox with splash lubrication," *Applied Sciences*, vol. 11, no. 1, pp. 352, 2020, doi: 10.3390/app11010352.
- [15] S. Chiranth, X. Yang and S. Jeff, "Conjugate heat transfer CFD analysis of an oil cooled automotive electrical motor," *SAE Int. J. Adv. & Curr. Prac. in Mobility*, vol. 2, no. 4, pp. 1741-1753, 2020, doi: 10.4271/2020-01-0168.
- [16] X. Zhu, Y. Dai and F. Ma, "CFD modelling and numerical simulation on windage power loss of aeronautic high-speed spiral bevel gears," *Simulation Modelling Practice and Theory*, vol. 103, pp. 102080:1-21, 2020, doi: 10.1016/j.simpat.2020.102080.
- [17] M.N. Mastrone, E.A. Hartono and V. Chernoray, "Oil distribution and churning losses of gearboxes experimental and numerical analysis," *Tribology International*, vol. 151, no. 106496, pp. 1-7, 2020, doi: 10.1016/j.triboint.2020.106496.
- [18] A. Hidenori, I. Hideyuki and N. Motohiko, "Computational fluid dynamics simulations and experiments for reduction of oil churning loss and windage loss in aeroengine transmission gears," *Journal of Engineering for Gas Turbines and Power*, vol. 136, no. 9, pp. 092604, 2014, doi: 10.1115/1.4026952.
- [19] A. Hidenori, I. Hideyuki and N. Motohiko, "Computational fluid dynamics simulations and experiments for reduction of oil churning loss and windage loss in aeroengine transmission gears," *Journal of Engineering for Gas Turbines and Power*, vol. 136, no. 9, pp. 092604, 2014, doi: 10.1115/1.4026952.
- [20] S. Shao, K. Zhang and Y. Yao, "Investigations on lubrication characteristics of high-speed electric multiple unit gearbox by oil volume adjusting device," *Journal of*

- Zhejiang University-SCIENCE A*, vol. 23, no. 12, pp. 1013-1026, 2023, doi: 10.1631/2023.A2200274.
- [21] H. Liu, J. Thomas and L. Thomas, "Determination of oil distribution and churning power loss of gearboxes by finite volume CFD method," *Tribology International*, vol. 109, pp. 346-354, 2016, doi: 10.1016/j.triboint.2016.12.042.
- [22] W. Li, and D.Q. Pang, "Investigation on temperature field of surrounding tooth domain with cracked tooth in gear system," *Mechanism and Machine Theory*, vol. 130, pp. 523-538, 2018, doi: 10.1016/j.mechmachtheory.2018.09.002.
- [23] Y.Z. Wang, W. Tang and Y.Y. Chen, "Investigation into the meshing friction heat generation and transient thermal characteristics of spiral bevel gears," *Applied Thermal Engineering*, vol. 119, pp. 245-253, 2017, doi: 10.1016/j.applthermaleng.2017.03.071.
- [24] L. Gan, K. Xiao, and J.X. Wang, "A numerical method to investigate the temperature behavior of spiral bevel gears under mixed lubrication condition," *Applied Thermal Engineering*, vol. 147, pp. 866-875, 2019, doi: 10.1016/j.applthermaleng.2018.10.125.
- [25] C. Pany, "Cylindrical shell pressure vessel profile variation footprint in strain comparison of test data with numerical analysis," *Liquid and Gaseous Energy Resources*, vol. 1, no. 2, pp. 91-101, doi:10.21595/lger.2021.22163.
- [26] A. Vamsi, J. Ansari, C. Pany et.al., "Structural design and testing of pouch cells," *Journal of Energy Systems*, vol. 5, no. 2, pp. 2602-2052, 2021, doi:10.30521/jes.815160
- [27] S. Sharma, C. Pany, R. Suresh, et.al., "Spiral Wound Gasket in a Typical Liquid Engine Convergent-Divergent Nozzle," *Advances in Thermal Sciences*, 2023, pp. 187-201, doi:10.1007/978-981-19-6470-1_16.